Bridging perturbation theory and simulations: initial conditions and fast integrators for cosmological simulations

Oliver Hahn[1,2⋆],

1 Institute for Astronomy, University of Vienna, Türkenschanzstraße 17, Vienna 1180, Austria
2 Department of Mathematics, University of Vienna, Oskar-Morgenstern-Platz 1, Vienna 1090, Austria

⋆ oliver.hahn@univie.ac.at

Abstract

These lecture notes provide an introduction to the generation of initial conditions for cosmological N-body simulations. Starting from the definition and properties of Gaussian random fields, we discuss their role in cosmology and the efficient generation of such fields using Fourier methods. The Vlasov-Poisson system is introduced as the governing framework for cold collisionless matter, and its solution via characteristics and Lagrangian perturbation theory (LPT) is detailed. We discuss the use of LPT for initializing N-body simulations, emphasizing the importance of high-order LPT and late-time starts to minimize truncation and discreteness errors. Finally, we discuss time integration schemes, including PT-informed integrators, and their role in accurately evolving the system. These notes aim to bridge the gap between theoretical perturbation methods and practical simulation techniques.

Received Date
Accepted Date
Published Date

Contents

1 Simulating Gaussian random fields

1.1 Definitions and properties

Gaussian random fields (GRFs, [1]) are the starting point for all cosmological simulations as they are (1) very simple objects to work with, and (2) very well motivated by observations of the CMB (which is extremely close to a GRF although deviations from perfect Gaussianity are much sought for).

Definition 1 (Gaussian random field, GRF). *A Gaussian random field (GRF) f is a random variable parameterised over a domain $\mathcal{D} \subset \mathbb{R}^d$ such that for any finite set of points $\boldsymbol{x}_1, \dots, \boldsymbol{x}_n \in \mathcal{D}$, the random variables $f(\boldsymbol{x}_1), \dots, f(\boldsymbol{x}_n)$ are jointly Gaussian distributed. The joint distribution is fully specified by the mean $\mu(\boldsymbol{x})$ and the covariance matrix $C(\boldsymbol{x}, \boldsymbol{y})$, i.e.*

$$\mathbb{E}[f(\boldsymbol{x})] = \mu(\boldsymbol{x}) \,, \qquad \mathbb{E}[f(\boldsymbol{x})f(\boldsymbol{y})] = C(\boldsymbol{x}, \boldsymbol{y}) + \mu(\boldsymbol{x})\mu(\boldsymbol{y}) \,. \tag{1}$$

*We call f **centered** if $\mu(\boldsymbol{x}) \equiv 0$ (which can always be achieved by re-defining the field as $f - \mu$). For a centered field, we call f **homogeneous** (or stationary) if the covariance is translation-invariant, i.e. if a function $\mathscr{C}$ exists so that*

$$C(\boldsymbol{x}, \boldsymbol{y}) = \mathscr{C}(\boldsymbol{x} - \boldsymbol{y}) \tag{2}$$

*and additionally **isotropic** if it is also rotation-invariant, i.e. if a ξ exists so*

$$C(\boldsymbol{x}, \boldsymbol{y}) = \xi(\|\boldsymbol{x} - \boldsymbol{y}\|) \,. \tag{3}$$

Theorem 1 (Isserlis/Wick). *Let $(f_1, \dots, f_n) := (f(\boldsymbol{x}_1), \dots, f(\boldsymbol{x}_n))$ be an n-variate Gaussian random variable with* zero mean *(i.e. centered), then*

$$\mathbb{E}[f_1 f_2 \dots f_n] = \begin{cases} \sum_{p \in P_n^2} \prod_{\{i,j\} \in p} \underbrace{\mathbb{E}[f_i f_j]}_{= \mathsf{C}(\boldsymbol{x}_i, \boldsymbol{x}_j)} & \text{if } n \text{ is even} \\ 0 & \text{if } n \text{ is odd} \end{cases} \tag{4}$$

where the sum is over all distinct partitions p of $\{1, \dots, n\}$ into pairs $\{i, j\}$, and the product is over the pairs in p. The proof can be found in all textbooks on statistics.

The meaning of the theorem is that the expectation value of the product of an even number of centered Gaussian random variables can always be expressed in terms of the covariance matrix C, while the expectation value of an odd number of centered Gaussian random variables vanishes. I.e. for a Gaussian field, the three-point correlator vanishes and the four-point correlator can be expressed in terms of two-point correlators, and so on. Conversely, for a non-Gaussian field, this is not true and can be used to quantify deviations from Gaussianity (e.g. through a non-vanishing three-point correlator).

1.2 Diagonality of covariance in Fourier space, sampling

Theorem 2 (Diagonality in Fourier space)**.** *A GRF is a GRF irrespective of the basis in which it is represented. In particular, the Fourier transform of a GRF is also a GRF, i.e.*

$$\hat{f}(\boldsymbol{k}) = \int_{\mathbb{R}^d} d^d x \; e^{-i\boldsymbol{k}\cdot\boldsymbol{x}} f(\boldsymbol{x}) \,, \tag{5}$$

is a complex GRF (where both the real and the imaginary part are GRFs). The corresponding covariance function in Fourier space of a centered homogeneous GRF is given by

$$\mathbb{E}[\hat{f}(\boldsymbol{k})\hat{f}^*(\boldsymbol{k}')] = (2\pi)^d \delta_D(\boldsymbol{k}-\boldsymbol{k}')\mathscr{P}(\boldsymbol{k}) \,, \tag{6}$$

where $\mathscr{P}(\boldsymbol{k})$ is the power spectrum. If the GRF is isotropic, then $\mathscr{P}(\boldsymbol{k}) = P(\|\boldsymbol{k}\|)$. Note that for real valued fields the Hermitian property holds, i.e. $\hat{f}^*(\boldsymbol{k}) = \hat{f}(-\boldsymbol{k})$, i.e. equivalently the form $\mathbb{E}[\hat{f}(\boldsymbol{k})\hat{f}(\boldsymbol{k}')] = (2\pi)^d \delta_D(\boldsymbol{k}+\boldsymbol{k}')\mathscr{P}(\boldsymbol{k})$ holds.

Proof. To prove the theorem, the covariance function in Fourier space is defined as:

$$\mathbb{E}[\hat{f}(\boldsymbol{k})\hat{f}^*(\boldsymbol{k}')] = \int_{\mathbb{R}^d} \mathrm{d}^d x \int_{\mathbb{R}^d} \mathrm{d}^d y \; e^{-\mathrm{i}(\boldsymbol{k}\cdot\boldsymbol{x}-\boldsymbol{k}'\cdot\boldsymbol{y})} \mathbb{E}[f(\boldsymbol{x})f(\boldsymbol{y})].$$

Using the definition of the covariance function in real space, $\mathbb{E}[f(\boldsymbol{x})f(\boldsymbol{y})] = C(\boldsymbol{x},\boldsymbol{y})$, and substituting $C(\boldsymbol{x},\boldsymbol{y}) = \mathscr{C}(\boldsymbol{x}-\boldsymbol{y})$ for homogeneous GRFs, we rewrite

$$= \int_{\mathbb{R}^d} \mathrm{d}^d x \int_{\mathbb{R}^d} \mathrm{d}^d y \; e^{-\mathrm{i}(\boldsymbol{k}\cdot\boldsymbol{x}-\boldsymbol{k}'\cdot\boldsymbol{y})} \mathscr{C}(\boldsymbol{x}-\boldsymbol{y}).$$

Changing variables to $\boldsymbol{r} = \boldsymbol{x}-\boldsymbol{y}$ and $\boldsymbol{X} = \boldsymbol{x}$, we have $\mathrm{d}^d x \mathrm{d}^d y = \mathrm{d}^d X \mathrm{d}^d r$. The integral becomes

$$= \int_{\mathbb{R}^d} \mathrm{d}^d X \int_{\mathbb{R}^d} \mathrm{d}^d r \; e^{-\mathrm{i}(\boldsymbol{k}-\boldsymbol{k}')\cdot\boldsymbol{X}} e^{-\mathrm{i}\boldsymbol{k}\cdot\boldsymbol{r}} \mathscr{C}(\boldsymbol{r}).$$

The integral over $\boldsymbol{X}$ yields a Dirac delta function: $\int_{\mathbb{R}^d} \mathrm{d}^d X \; e^{-\mathrm{i}(\boldsymbol{k}-\boldsymbol{k}')\cdot\boldsymbol{X}} = (2\pi)^d \delta_D(\boldsymbol{k}-\boldsymbol{k}')$. Substituting this result, we finally obtain the key result

$$\mathbb{E}[\hat{f}(\boldsymbol{k})\hat{f}^*(\boldsymbol{k}')] = (2\pi)^d \delta_D(\boldsymbol{k}-\boldsymbol{k}') \int_{\mathbb{R}^d} \mathrm{d}^d r \; e^{-\mathrm{i}\boldsymbol{k}\cdot\boldsymbol{r}} \mathscr{C}(\boldsymbol{r}).$$

This completes the proof. The remaining integral is the Fourier transform of the covariance function $\mathscr{C}(\boldsymbol{r})$, which defines the power spectrum $\mathscr{P}(\boldsymbol{k})$

$$\mathscr{P}(\boldsymbol{k}) := \int_{\mathbb{R}^d} \mathrm{d}^d r \; e^{-\mathrm{i}\boldsymbol{k}\cdot\boldsymbol{r}} \mathscr{C}(\boldsymbol{r}).$$

For a homogeneous and isotropic field of course there exists a P so that $\mathscr{P}(\boldsymbol{k}) = P(\|\boldsymbol{k}\|)$. □

We can therefore generate a centered homogenous and isotropic GRF by sampling in the diagonal Fourier eigenbasis, i.e.

$$\hat{f}_j = \sqrt{P(\|\boldsymbol{k}_j\|)} \, \frac{\alpha_j + \mathrm{i}\beta_j}{\sqrt{2}} \qquad \alpha_j, \beta_j \sim \mathcal{N}(0,1), \tag{7}$$

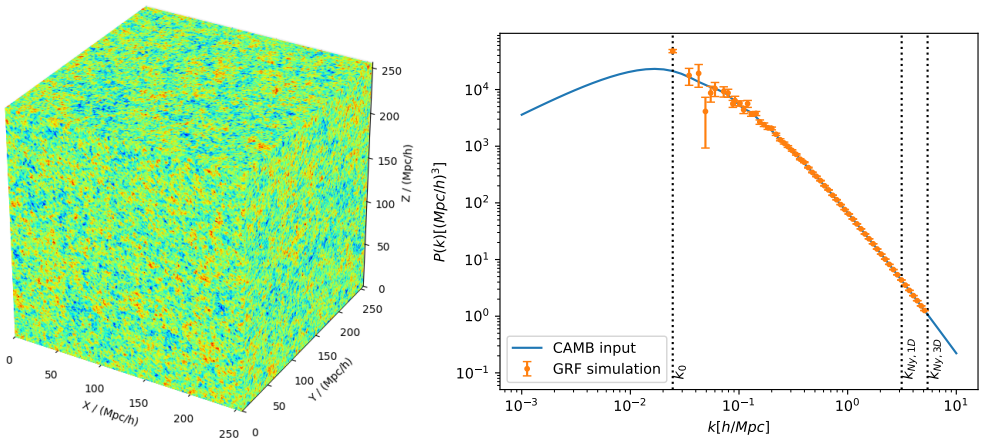

Figure 1: Left: Realization of a Gaussian random field in a cubic periodic domain $\mathcal{D} = \mathbb{T}^3$. Right: Corresponding isotropically averaged power spectrum of the field realisation along with the input expectation value obtained with CAMB. The vertical lines indicate the fundamental mode of the box $2\pi/L$ and the 1D and 3D Nyquist mode $N\pi/L$, and $\sqrt{3}N\pi/L$.

then it is easy to verify that $\mathbb{E}[\hat{f}_j \hat{f}_j^*] = P(\|\boldsymbol{k}_j\|)$. The basis vectors are given by the Fourier basis $\hat{v}_j(\boldsymbol{x}) = \mathrm{e}^{\mathrm{i}\boldsymbol{k}_j\cdot\boldsymbol{x}}$ and $P(k)$ is a given isotropic power spectrum, obtained usually from an Einstein-Boltzmann code such as CAMB[1] or CLASS[2]. The full field in real space is then realised by linear combination (effectively just an inverse discrete Fourier transform)

$$f(\boldsymbol{x}) = \mathrm{Re} \sum_j \hat{f}_j \mathrm{e}^{\mathrm{i}\boldsymbol{k}_j\cdot\boldsymbol{x}} \tag{8}$$

where we took the real part since we since without additional constraints on the coefficients, the resulting field would be complex. Alternatively, one could require the coefficients to obey a Hermitian symmetry, i.e. that $\hat{f}(\boldsymbol{k}_j) = \hat{f}^*(-\boldsymbol{k}_j)$. In practice this can be efficiently computed using the Fast Fourier Transform (FFT). In particular, given the matter power spectrum $P_m(k)$, a realisation of the primordial density field $\delta(\boldsymbol{k})$ can be made in a few lines of code, as shown in Figure 1, you can try it out yourself in the accompanying notebook, where a field is sampled from all modes representable on a periodic domain (3-torus) up to a given resolution dependent Nyquist frequency.

2 The dynamics of cold collisionless matter

2.1 Definitions, the cosmological Vlasov-Poisson system

On large enough scales and at late times, the evolution of cosmic matter on sub-horizon scales can be described as that of a cold collisionless fluid evolving under its Newtonian self-gravity. Assume the one-particle phase space is given by $\mathcal{P} := \mathcal{D} \times \mathbb{R}^3 \times [0, T]$, where $\mathcal{D} \subset \mathbb{R}^3$ is usually a 3-torus (periodic box) $\mathbb{T}^3$. For simplicity we normalise the volume so that $\int_{\mathcal{D}} \mathrm{d}^3x = 1$. The density in phase space of matter is given by a positive definite density $f(\boldsymbol{x}, \boldsymbol{v}, t) \geq 0$ and we want to describe the fluid in terms of the evolution of this density function. Such a system is described by the cosmological Vlasov-Poisson (VP) equations, see e.g. [2–4] for more details.

[1] CAMB is available from https://camb.info
[2] CLASS is available from http://class-code.net

Definition 2 (Cosmological VP system). *In comoving coordinates, the VP equations are given by*

$$\frac{\partial f}{\partial t} + \frac{\boldsymbol{v}}{a^2}\cdot\boldsymbol{\nabla}_x f - \boldsymbol{\nabla}_x\phi\cdot\boldsymbol{\nabla}_v f = 0 \tag{9a}$$

$$\nabla_x^2\phi + \frac{\kappa}{a}(1-n) = 0 \qquad n := \int_{\mathbb{R}^3} f\, d^3v \quad \textit{and} \quad \int_{\mathcal{D}} n\, d^3x = 1 \tag{9b}$$

where $\kappa := 3H_0^2\Omega_m/2$. The 'scale factor' $a(t)$ is the solution to a Friedmann equation $\dot{a} = aH(a)$ where $H(a)$ is the Hubble function, and e.g. for a flat ΛCDM universe

$$H(a) = \sqrt{\Omega_m a^3 + (1-\Omega_m)}\,. \tag{9c}$$

Since the fluid is cold, it has (initially) no extent in velocity space at fixed location and we specify the initial data solely in terms of an initial velocity perturbation, i.e. at $t = 0$, we set for a cold fluid

$$f(\boldsymbol{x},\boldsymbol{v},t_0) = \delta_D(\boldsymbol{v} - \boldsymbol{v}_0(\boldsymbol{x}))\,. \tag{9d}$$

Eqs.(9a)-(9d) constitute a rather non-trivial set of non-linear partial differential equations and we typically have to resort to numerical or perturbative solutions to arrive at approximate solutions for general initial data.

2.2 Solution by method of characteristics

The Vlasov equation (9a) can be solved by the method of characteristics. Characteristics are a family of one-parameter curves $\boldsymbol{X}(t), \boldsymbol{V}(t)$ in phase space that transport the initial data across space and time. They are defined as the solutions to the characteristic ordinary differential equations (ODEs). The total derivative of the phase space density f along the characteristic curves is given by

$$\frac{\mathrm{d}}{\mathrm{d}t} f(\boldsymbol{X}(t),\boldsymbol{V}(t),t) = \frac{\partial f}{\partial t} + \dot{\boldsymbol{X}}\cdot\boldsymbol{\nabla}_x f + \dot{\boldsymbol{V}}\cdot\boldsymbol{\nabla}_v f\,. \tag{10}$$

Clearly, the phase space density f is conserved along the characteristic curves, i.e. $\mathrm{d}f/\mathrm{d}t = 0$, if the characteristic ODEs are chosen such that

$$\dot{\boldsymbol{X}} = \frac{\boldsymbol{V}}{a^2}\,, \qquad \dot{\boldsymbol{V}} = -(\boldsymbol{\nabla}_x\phi)(\boldsymbol{X})\,. \tag{11}$$

equivalent to the second order ODE

$$\ddot{\boldsymbol{X}} = -2H\dot{\boldsymbol{X}} - \frac{1}{a^2}(\boldsymbol{\nabla}_x\phi)(\boldsymbol{X})\,. \tag{12}$$

The solution is fully determined once the initial data (9d), i.e. $\boldsymbol{X}(0) = \boldsymbol{q}$ and $\boldsymbol{V}(0) = \boldsymbol{v}_0(\boldsymbol{q})$ is specified for all $\boldsymbol{q} \in \mathcal{D}$. The density n can be shown to be related to the conservation of the measure

$$n\,\mathrm{d}^3x = \mathrm{d}^3q \qquad \Leftrightarrow \qquad n(\boldsymbol{X},t)\left|\frac{\partial \boldsymbol{X}}{\partial \boldsymbol{q}}\right| = 1\,, \tag{13}$$

where we often write the Jacobian determinant as J, i.e. $n = 1/|J|$ so that the formal solution to the Poisson equation (9b) is given by

$$\phi(\boldsymbol{X},t) = \frac{\kappa}{a}\boldsymbol{\nabla}_X^{-2}\frac{J-1}{J}\,. \tag{14}$$

We will leave this formal result as it is for now, and consider perturbative solutions later.

Definition 3 (Shell-crossing singularity). *For a fluid with cold initial data, there can (and generally will) be a time t_* when the mapping $\boldsymbol{q} \mapsto \boldsymbol{X}(\boldsymbol{q}, t_*)$ becomes multi-valued and thus no longer one-to-one. This is accompanied by a vanishing of the Jacobian J of the map, leading to a formal divergence of the density $n = 1/J$.*

2.3 Cosmological Euler-Poisson via the Boltzmann hierarchy

The integrating out of velocity degrees of freedom when going from the phase space density f to the configuration space density n can be applied systematically by performing an expansion of f in terms of the Boltzmann hierarchy of moments of the distribution function

$$n(\boldsymbol{x},t) := \int_{\mathbb{R}^3} f(\boldsymbol{x},\boldsymbol{v},t)\,\mathrm{d}^3v\,; \quad n\boldsymbol{u} := \int \boldsymbol{v} f\,\mathrm{d}^3v\,; \quad n(\boldsymbol{\sigma}+\boldsymbol{u}\otimes\boldsymbol{u}) := \int \boldsymbol{v}\otimes\boldsymbol{v} f\,\mathrm{d}^3v\,, \quad \dots\,, \tag{15}$$

which correspond to density, momentum density, and total energy tensor, and we omitted the explicit function arguments for the second two expressions. The same expansion in terms of moments can be applied, which yields an infinite hierarchy of equations, the first of which are the only ones we shall consider here.

Definition 4 (Cosmological Euler-Poisson system)**.** *The first two marginals of the Boltzmann hierarchy correspond to the cosmological Euler-Poisson system (cf. [2])*

$$\frac{\partial n}{\partial t} + \frac{1}{a^2}\boldsymbol{\nabla}_x\cdot(n\boldsymbol{u}) = 0 \tag{16a}$$

$$\frac{\partial \boldsymbol{u}}{\partial t} + \frac{1}{a^2}(\boldsymbol{u}\cdot\boldsymbol{\nabla}_x)\boldsymbol{u} = -\boldsymbol{\nabla}_x\phi - \frac{1}{na^2}\boldsymbol{\nabla}_x\cdot(n\boldsymbol{\sigma}) \tag{16b}$$

supplemented with the Poisson equation (9b) *from above.*

With initial data given by (9d), the respective initial data for the hierachy becomes

$$n(\boldsymbol{x},0) = 1, \qquad \boldsymbol{u}(\boldsymbol{x},0) = \boldsymbol{v}_0(\boldsymbol{x}), \qquad \boldsymbol{\sigma}(\boldsymbol{x},0) = 0\,. \tag{16c}$$

In the cold limit, one thus has $\boldsymbol{\sigma} = 0$ initially, and the system is closed. However, even if $\boldsymbol{\sigma} = 0$ initially, internal anistropic stress will be generated (non-perturbatively) during shell-crossing. Before shell-crossing, the term $\boldsymbol{\sigma}$ can however be assumed to vanish everywhere and thus dropped from the equation.

You have learned in the introductory lectures that equations (16a)-(16b) plus the Poisson equation can be solved perturbatively by defining $\delta := n-1$ as a small parameter. At first order (of the standard perturbation theory) one has the well known result

$$\delta(\boldsymbol{x},t) = D_+(t)\,\delta_+(\boldsymbol{x}) + D_-(t)\,\delta_-(\boldsymbol{x})\,, \tag{17}$$

i.e. the linear solution separates into a growing and a decaying mode, where $D = D_\pm$ solve the so-called linear 'Eulerian perturbation equation'

$$\ddot{D} + 2H\dot{D} - \frac{3}{2}H_0^2\Omega_m\frac{D}{a^3} = 0. \tag{18}$$

and the spatial pieces $\delta_\pm(\boldsymbol{x})$ are determined by the initial condition. In the case of a flat ΛCDM universe, one has [5]

$$D_+ = a\sqrt{1+\lambda_0\,a^3}\;{}_2F_1\left(\frac{3}{2},\frac{5}{6},\frac{11}{6},-\lambda_0\,a^3\right), \qquad D_- = a^{-3/2}\sqrt{1+\lambda_0\,a^3}, \tag{19}$$

where ${}_2F_1$ is Gauss' hypergeometric function, and $\lambda_0 := (1-\Omega_m)/\Omega_m$. In Newtonian gravity, for a cold fluid, linear growth is thus completely scale-independent. This is of course not true in relativistic perturbation theory, since the *horizon scale* introduces a physical scale with sub- and super-horizon scales obeying different growth rates. In the presence of finite temperature effects, another scale, the *Jeans scale*, enters below which the growth of perturbations is suppressed.

2.4 Vlasov early time asymptotics: Zel'dovich approximation

A particularly useful result can be obtained by expressing the Vlasov equation (9a) using the growth function D_+ as the time variable. This works of course as long as there is a monotonous relation between t and D_+. Defining a new, re-scaled, velocity $\boldsymbol{w} := \frac{\boldsymbol{v}}{a^2\dot{D}_+}$, one can re-write the Vlasov-Poisson system for $a \to 0$ as

$$\frac{\partial f}{\partial D} + \boldsymbol{w}\cdot\boldsymbol{\nabla}_x f - \frac{\kappa D}{a^3\dot{D}^2}(\boldsymbol{w}+\boldsymbol{\nabla}\varphi)\cdot\boldsymbol{\nabla}_w f = 0\,. \qquad \nabla_X^2\varphi - \frac{\delta}{D} = 0 \tag{20}$$

where the potentials are related as $\varphi = \frac{a}{\kappa D}\phi$. The characteristic ODEs can again be combined into a single second order ODE, defining the growth rate $f := \mathrm{d}\log D/\mathrm{d}\log a$,

$$\boldsymbol{X}' = \boldsymbol{W}\,, \qquad \boldsymbol{W}' = -\frac{\kappa D}{a^3\dot{D}^2}(\boldsymbol{W}+\boldsymbol{\nabla}_X\varphi)\,, \tag{21}$$

$$\Leftrightarrow \qquad \boldsymbol{X}'' = -\frac{\kappa}{a^3 f^2 H^2 D}\left(\boldsymbol{X}' + \boldsymbol{\nabla}_X\varphi\right)\,. \tag{22}$$

where a prime now denotes the derivative with respect to D. To find an asymptotic solution for early times, we can use the fact that the growth factor D is given by $D \asymp a$ in the matter dominated era of ΛCDM, so that the whole prefactor has the following early time asymptotic behaviour, allowing to determine the asymptotic form of the characteristic ODE

$$\frac{\kappa}{a^3 f^2 H^2 D} \asymp \frac{3}{2a} \qquad \Rightarrow \qquad \boldsymbol{X}' + \boldsymbol{\nabla}\varphi = \frac{2a}{3}\boldsymbol{X}'' \overset{a\to 0}{\to} 0\,. \tag{23}$$

Therefore asymptotically, the characteristics are given by the asymptotic solution for $a \to 0$ in terms of the initial velocity perturbation $\boldsymbol{W}_0 = -\boldsymbol{\nabla}_q\varphi_0$ as [6]

$$\boldsymbol{X}_0 = \boldsymbol{q} \qquad \boldsymbol{X}_0' = -\boldsymbol{\nabla}\varphi_0(\boldsymbol{q}) \qquad \Rightarrow \qquad \boldsymbol{X} = \boldsymbol{q} - D_+\,\boldsymbol{\nabla}\varphi_0(\boldsymbol{q}) + \mathcal{O}(D_+^2)\,, \tag{24}$$

This is the Zel'dovich approximation (ZA, [7]): at leading order, characteristics are straight lines in D_+-time (only the D_+ branch is finite as $a \to 0$) with the slope of the line set by $\boldsymbol{\nabla}\varphi_0$.

2.5 Lagrangian perturbation theory

We first write the characteristic solution for the position in terms of the initial (so-called Lagrangian) coordinate and a displacement relative to it as

$$\boldsymbol{X}(\boldsymbol{q},t) = \boldsymbol{q} + \boldsymbol{\Psi}(\boldsymbol{q},t) \tag{25}$$

The Jacobian matrix J of this coordinate change is in index notation given by

$$(\mathsf{J})_{ij} = \frac{\partial X_i}{\partial q_j} = \delta_{ij} + \psi_{i,j} \qquad \Rightarrow \qquad \boldsymbol{\nabla}_X = \mathsf{J}^{-1}\cdot\boldsymbol{\nabla}_q \qquad \text{and} \qquad J = \det\mathsf{J}\,. \tag{26}$$

We first write eq. (22) in slightly more concise form inserting the Poisson equation as

$$\mathfrak{D}\boldsymbol{X} = \boldsymbol{\nabla}_X\nabla_X^{-2}\left(1-\frac{1}{J}\right) \qquad \text{where} \qquad \mathfrak{D} := \frac{a^3}{\kappa}\left(\frac{\mathrm{d}^2}{\mathrm{d}t^2} + 2H\frac{\mathrm{d}}{\mathrm{d}t}\right) \tag{27}$$

and next we hit this equation with another $\boldsymbol{\nabla}_X$ to decompose it into a longitudinal and a transversal part, i.e. in index notation

$$\frac{\partial q_j}{\partial X_i}\mathfrak{D}\frac{\partial X_i}{\partial q_j} = 1 - \frac{1}{J} \qquad \text{and} \qquad \epsilon_{ijk}\frac{\partial q_l}{\partial X_j}\mathfrak{D}\frac{\partial X_k}{\partial q_l} = 0 \tag{28}$$

The second equation expresses the conservation of vorticity, but since we must assume that the vorticity is zero initially (vorticity is a decaying mode), we can directly impose the stronger constraint that $\boldsymbol{\nabla}_X \times \frac{\mathrm{d}\boldsymbol{X}}{\mathrm{d}t} = 0$. Here, we will neglect the transversal part entirely as it only enters at third order of the perturbation theory and focus on the longitudinal modes exclusively.

We now make a weak perturbative ansatz of the form

$$\boldsymbol{X} = \boldsymbol{q} + \epsilon D_1(t)\boldsymbol{\nabla}_q \phi^{(1)} + \epsilon^2 D_2(t)\boldsymbol{\nabla}_q \phi^{(2)} + \dots \tag{29a}$$

$$\Rightarrow \qquad \mathsf{J} = \mathsf{I} + \epsilon \mathsf{A} \qquad \text{with} \quad (\mathsf{A})_{ij} = D_1(t)\phi^{(1)}_{,ij} + \epsilon D_2(t)\phi^{(2)}_{,ij} + \dots \tag{29b}$$

In three dimensions, the following formula holds for the determinant of a 3×3 matrix $\mathsf{I}+\epsilon\mathsf{A}$:

$$\begin{aligned} J = \det \mathsf{J} = \det(\mathsf{I}+\epsilon\mathsf{A}) &= 1 + \epsilon\,\mathrm{Tr}(\mathsf{A}) + \frac{\epsilon^2}{2}\left(\mathrm{Tr}(\mathsf{A})^2 - \mathrm{Tr}(\mathsf{A}^2)\right) + \epsilon^3 \det \mathsf{A}\,, \\ &=: 1 + \epsilon\mu_1(\mathsf{A}) + \epsilon^2\mu_2(\mathsf{A}) + \epsilon^3\mu_3(\mathsf{A})\,. \end{aligned} \tag{29c}$$

and therefore

$$1 - \frac{1}{J} = \epsilon\,\mu_1 - \epsilon^2\left(\mu_1^2 - \mu_2\right) + \epsilon^3\left(\mu_1^3 - 2\mu_1\mu_2 + \mu_3\right) + O(\epsilon^4)\,. \tag{29d}$$

The von Neumann series of the inverse of a matrix allows us to write

$$\mathsf{J}^{-1} = (\mathsf{I}+\epsilon\mathsf{A})^{-1} = \sum_{n=0}^{\infty}(-\epsilon)^n\mathsf{A}^n = \mathsf{I} - \epsilon\mathsf{A} + \epsilon^2\mathsf{A}^2 - \dots\,, \tag{29e}$$

First order solution (1LPT=ZA). Keeping all terms to first order in ϵ, we find

$$(\mathfrak{D}-1)\,D_1\phi^{(1)}_{,ii} = 0 \qquad \Rightarrow \qquad (\mathfrak{D}-1)\,D^{(1)} = 0 \tag{30}$$

which is unsurprisingly the same as the linear Eulerian PT eq. (18), so $D_1 = D_+$ and $\phi^{(1)}_{,ii} = \delta_+$. And with initial data $\phi^{(1)} = -\varphi^{\mathrm{ini}}$ this yields of course the Zel'dovich approximation

$$\boldsymbol{X} = \boldsymbol{q} - D_+\boldsymbol{\nabla}_q\varphi^{\mathrm{ini}}. \tag{31}$$

Note that if the initial data φ^{ini} is planar one-dimensional, then all higher order LPT terms vanish, and the Zel'dovich approximation is actually exact (until shell-crossing).

Second order solution (2LPT). Keeping terms of order ϵ^2 we find (since $\mathfrak{D}D_1 = D_1$)

$$\mathfrak{D}D_2\phi^{(2)}_{,ii} = -D_1^2\mu_2(\phi^{(1)}_{,ij})\,. \tag{32}$$

Equating the temporal and the spatial pieces separately, one has [8,9]

$$(\mathfrak{D}-1)\,D_2 = -D_1^2 \qquad \text{and} \qquad \phi^{(2)} = \nabla_q^{-2}\tfrac{1}{2}\left(\phi^{(1)}_{,ij}\phi^{(1)}_{,ij} - \phi^{(1)}_{,ii}\phi^{(1)}_{,jj}\right) \tag{33}$$

The ODE for the second order growth function $D^{(2)}$ has to be integrated numerically usually. If few per cent level accuracy is enough, the following asymptotic form can be used [9]

$$D_2 \approx -\frac{3}{7}\Omega_m^{-2/63}D_1^2\,. \tag{34}$$

All-order recursion relations (nLPT). It is possible to determine all order recursion relations for LPT without too much further effort from the master equations (28) [10–12]. These allow to compute the $n+1$-th order based on the previous orders up to n. In the left panel of Figure 2, the contributions $\|\psi^{(n)}\|$ for GRF initial conditions are shown (see also [13]). The slowest convergent pieces are close to spherically expanding/collapsing regions. When computing the nLPT series for spherical collapse (see lectures by Cora Uhlemann), one sees that even in the underdense case, the convergence of the nLPT perturbative expansion is limited by the shell-crossing singularity which defines the conergence radius. This means that we can safely approach the regime just before shell-crossing singularities appear using high order LPT, but have to resort to N-body simulations to go beyond shell-crossing. Equations up to 3LPT can be found e.g. in [14], an implementatio recipe for $nLPT$ recursion in the appendix of [13].

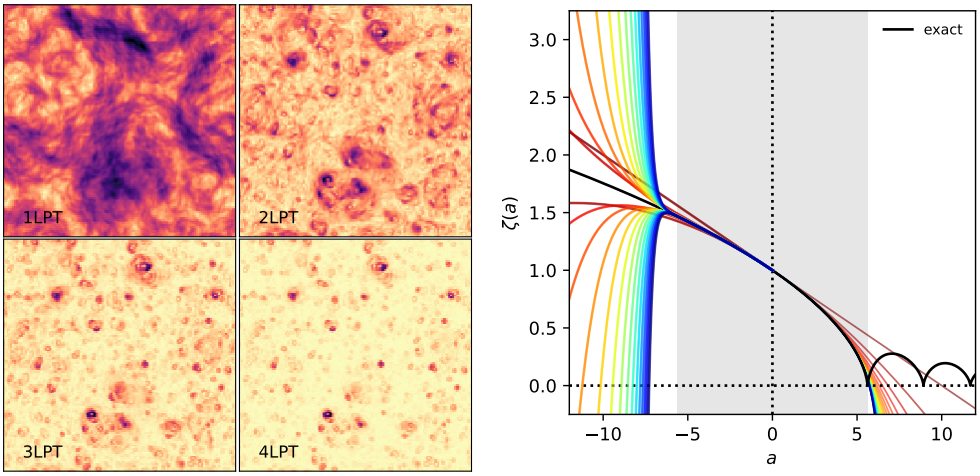

Figure 2: Left: Norm of the displacement field $\|\boldsymbol{\psi}^{(n)}\|$ as a function of the initial Lagrangian coordinate $\boldsymbol{q}$ up to 4LPT. The slowest converging regions are almost spherically collapsing and expanding regions. (Adapted from [13]) Right: Convergence from 1LPT to 30LPT to the trajectory of spherical collapse (black line) indicating the slow convergence. The radius of convergence in both the over and underdense case is determined by the shell-crossing singularity at $a_* = \frac{1}{2}(12\pi)^{2/3} \approx 5.6$.

3 N-body simulations and PT-informed time integration

As discussed above, nLPT is exceedingly accurate in the regime before shell-crossing singularities appear. To go beyond, one has to resort to N-body simulations.

3.1 N-body initial conditions

Ever since the some of the first cosmological N-body simulations in the 1980s, LPT has been used to initialize N-body simulations. Initially using 1LPT/ZA, increasing precision of simulations in the early 2000s [15] indicated that there can be 'transients' appearing when 1LPT is used. These are effectively truncation errors due to neglecting higher order LPT terms in the initial conditions. The simulation has to evolve for some time for the truncations errors to become small compared to the growth of non-linearities in the simulation itself – this is particularly true for higher order statistics such as 3-point functions and hiher. More recently [14] pointed out that for current precision requirements, it is best to use high-order LPT and an

as late as possible time to start the N-body simulation to reduce both truncation errors and discreteness effects (for the latter see subsection 3.4).

There is a mismatch in physics between what we include in the Einstein-Boltzmann solvers (linear but fully relativistic) and what we typically include in simulations of the late Universe (non-linear but non-relativistic). This is justified as we have a good separation of scales (in time and space) where these two are relevant: non-linearities are relevant only on scales much smaller than the horizon. This means that horizon-scale effects can be safely modeled using linear corrections if needed, and other post-Newtonian effects on small cosmological scales are of order $\sim 10^{-5}$ [16]. For all simulations that cover scales smaller than the horizon, relativistic effects can thus be safely neglected.

The steps to initialize an N-body simulation are thus

1. Compute a matter power spectrum $P_m(k)$ at a target redshift, e.g. $z_{\rm target} = 0$ using an Einstein-Boltzmann code (e.g. CAMB or CLASS)

2. Simulate a primordial potential φ_0 as a GRF with a spectrum $P_\varphi = k^{-4} P_m(k)/D_+(z_{\rm target})^2$

3. Compute the nLPT spatial terms and assemble the total displacement field to n-th order for each particle for growth factors $D_1, D_2, \ldots$ at $z_{\rm start}$

$$\boldsymbol{X}_i = \boldsymbol{q}_i + D_1 \boldsymbol{\psi}^{(1)}(\boldsymbol{q}) + D_2 \boldsymbol{\psi}^{(1)}(\boldsymbol{q}) + \ldots \tag{35}$$

   determine the initial particle velocity (careful about definition, which may be different for different N-body codes)

$$\boldsymbol{V}_i = \frac{\mathrm{d}\boldsymbol{X}_i}{\mathrm{d}t} = \dot{D}_1 \boldsymbol{\psi}^{(1)}(\boldsymbol{q}) + \dot{D}_2 \boldsymbol{\psi}^{(1)}(\boldsymbol{q}) + \ldots \tag{36}$$

   easiest achieved by placing $\boldsymbol{q}_i$ on a regular lattice. Note that the derivatives of the growth factors come for free when integrating the ODEs as they are second order.

4. Start your N-body simulation at $z_{\rm start}$ and evolve to whatever time you are interested in using time integration as explained next, and using Poisson solvers as explained in Romain Teyssier's lecture.

An example of how to carry out steps 1 to 3 can be found in a JUPYTER notebook accompanying these notes. Software that implements these steps includes e.g. 2LPTIC/N-GENIC[3] for 2LPT ICs, and MONOFONIC[4] for 3LPT ICs and for mult-fluid baryon+CDM ICs.

3.2 Standard time integrators

Based on the characteristic equations in cosmic time eqs. (11), it is natural to advance particles using a leapfrog scheme that advances (e.g. in drift-kick-drift form) [17] with $a_{n+1} - a_n = \Delta a$ to evolve positions and velocities for particle $i = 1, \ldots, N$ by one time step

$$\boldsymbol{X}_i^{n+1/2} = \boldsymbol{X}_i^n + \boldsymbol{V}_i^n \int_{a_n}^{a_{n+1/2}} \frac{\mathrm{d}a}{a^3 H} \,, \tag{37a}$$

$$\boldsymbol{V}_i^{n+1} = \boldsymbol{V}_i^{n+1} - \boldsymbol{\nabla}\Phi^{n+1/2} \int_{a_n}^{a_{n+1}} \frac{\mathrm{d}a}{a^2 H} \,, \tag{37b}$$

$$\boldsymbol{X}_i^{n+1} = \boldsymbol{X}_i^{n+1/2} + \boldsymbol{V}_i^{n+1} \int_{a_{n+1/2}}^{a_{n+1}} \frac{\mathrm{d}a}{a^3 H} \,. \tag{37c}$$

[3] The original 2LPTIC is available from https://cosmo.nyu.edu/roman/2LPT/, and N-GENIC which builds on it from https://www.h-its.org/2014/11/05/ngenic-code/

[4] MONOFONIC is available from https://github.com/cosmo-sims/monofonIC

This integrator can be proven to be second order accurate and symplectic (see [18] for definitions and properties of geometric integrators) . It is however non-optimal for cosmological simulations, as it can be shown to not reproduce the Zel'dovich solution for one-dimensional initial data exactly (even though that just consists of intertial motion!). The reason is that it uses poorly chosen time and velocity definitions for large-scale evolution. This can be formally quantified as follows.

Definition 5 (Zeldovich consistency)**.** *A time integrator is Zel'dovich consistent, if it reproduces the Zel'dovich solution* (31) *for one-dimensional data exactly in a single time step. See [19] for more details.*

3.3 PT-informed integrators

Instead of using the cosmic time velocity, we can employ the velocity we defined above that lead to the inertial Zel'dovich motion asymptotically, i.e. $\boldsymbol{W} := \boldsymbol{V}/F$ with $F := a^2\dot{D}$ so that

$$\boldsymbol{X}' = \boldsymbol{W} \,, \qquad \boldsymbol{W}' = -\frac{\kappa D}{a^3\dot{D}^2}\left(\boldsymbol{W} + \boldsymbol{\nabla}_X\varphi\right) \,, \tag{38}$$

Let us formulate a more general D-time integrator (again in drift-kick-drift form), where now one steps in D, i.e. $D_{n+1} - D_n = \Delta D$, as

$$\boldsymbol{X}_i^{n+1/2} = \boldsymbol{X}_i^n + \frac{\Delta D}{2}\boldsymbol{W}_i^n \tag{39a}$$

$$\boldsymbol{W}_i^{n+1} = \alpha\boldsymbol{W}_i^n + \frac{\beta}{D_{n+1/2}}\boldsymbol{\nabla}\varphi(\boldsymbol{X}_i^{n+1/2}) \tag{39b}$$

$$\boldsymbol{X}_i^{n+1} = \boldsymbol{X}_i^{n+1/2} + \frac{\Delta D}{2}\boldsymbol{W}_i^{n+1} \tag{39c}$$

Theorem 3 (Zel'dovich consistent time integrator)**.** *The integrator* (39) *is Zel'dovich consistent if the functions α and β are chosen such that*

$$\beta = 1 - \alpha \,. \tag{40}$$

The proof is straightforward and can be found in [19].

Multiple choices are thus possible as the class of Zel'dovich consistent integrators of the above form still allows the freedom to choose the function α.

Fast-PM For the 'FAST-PM' code, the first PT-informed integrator was proposed by [20]. Although it was not proven in the original paper, this integrator is symplectic and 2nd order, and thus the only flavour that is both symplectic and Zel'dovich consistent. For the integrator to be symplectic, the function α must be chosen to recover the 'canonical momentum' $\boldsymbol{V}_i$ at the end of the time step, i.e.

$$\alpha = \frac{F_n}{F_{n+1}} \,. \tag{41}$$

Bullfrog The BULLFROG integrator [21] abandons symplecticity but matches the trajectory to 2LPT. In order to achieve this, the coefficient α must be chosen as

$$\alpha = \frac{E'_{n+1} - G_{n+1/2}}{E'_n - G_{n+1/2}} \qquad \text{with} \qquad G_{n+1/2} := D_n^{-1}\left(E_n + E'_n\frac{\Delta D}{2}\right) - D_{n+1/2} \,, \tag{42}$$

where $E := D^{(2)}$ is the second order growth factor. This integrator produces the most accurate non-linear evolution on large scales with few time steps.

Clearly, in the limit of many time steps, all integrators should converge to the same solution. That solution will however be impacted by the quality of the force calculation (see lecture notes by Romain Teyssier).

3.4 Discretness effects in cosmological simulations

In this notes, we have derived two descriptions of non-linear structure formation as described by the Vlasov-Poisson system: the LPT perturbative approach, and the N-body simulation. The main difference is that in the N-body simulation, the Poisson source is approximated through the discrete characteristics, and re-expanded in each time step, while in nLPT the continuous evolution is computed order by order at the initial time. For the Poisson source one thus has

$$1+\delta_{\text{N-body}}(\boldsymbol{x},t) = \frac{1}{N}\sum_{i=1}^{N}\delta_D(\boldsymbol{x}-\boldsymbol{X}_t(t)) \tag{43a}$$

$$1+\delta_{\text{LPT}}(\boldsymbol{x},t) = J^{-1} \tag{43b}$$

It can be shown that at the particle scale, the N-body discretization leads to anisotropic deviations from the linear growth D_+. For simple cubic lattices, this deviation can be calculated exactly [22], and the ratio is shown in Figure 3 (left panel).

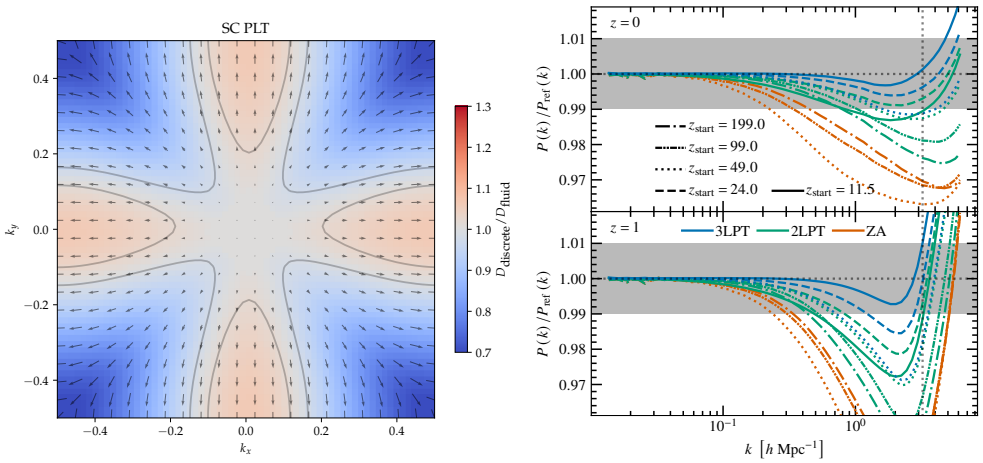

Figure 3: Left: Ratio of the growth factor of the discrete lattice system of particles to that of the fluid system in Fourier space. One clearly sees that the smallest modes $k \gtrsim k_{\text{Ny}}/2$ grow anisotropically and slower than in the fluid limit. Right: Error in the power spectrum at $z = 1$ and $z = 0$ depending on starting redshift of the N-body simulation and order of the LPT used to initialise it.

There are thus two competing numerical errors related to initial condition generation:

LPT truncation error As we are not using ∞LPT, there will be an error due to the truncation of the LPT expansion at finite order. This effect grows with time until shell-crossing appears and LPT becomes invalid. The error can be controlled by either starting the simulation at an earlier time, or by going to higher order LPT.

Discreteness errors Due to the particle discreteness effect in N-body simulations, error on small scales appear that are larger, the longer the simulation grows and the more linear it is. This error can be controlled by starting the 'discrete' evolution as late as possible, or by explicitly correcting for it [23].

The impact on the $z = 0$ and $z = 1$ non-linear power spectrum of these two competing effects can be seen in Figure 3 (right panel, adapted from [14]). The conclusion made in [14] from this analysis is that simulations are most accurately initialised with high order LPT at very late times, e.g. 3LPT at $z = 24$ in their analysis – which is quite in contrast to what was done before, where the common lore was that simulations should be initialised as early as possible.

4 Conclusion

In these lecture notes, we derived and discussed the main concepts and key aspects involved in generating initial conditions for cosmological N-body simulations from Gaussian random fields. The main take-aways are:

1. GRFs on periodic domains have diagonal covariance in Fourier space (the power spectrum $P(k)$), which allows very efficient simulation of GRFs with a given $P(k)$ using discrete Fourier transforms.

2. The Vlasov-Poisson system can be re-written in terms of ODEs for characteristic curves. In LPT, these characteristics are evolved in the continuum limit.

3. In first order LPT, characteristics correspond to straight lines parameterised by the linear growth D_+.

4. Higher order LPT can be constructed by building on top of first order.

5. LPT displacements and velocities can then be used as starting points for N-body simulations. Most efficient N-body simulations (in the mildly non-linear regime) use time integrators that integrate LPT evolution.

6. N-body simulations suffer from discreteness errors, which can be controlled by starting the simulations as late as possible, from LPT of sufficiently high order.

References

[1] R. J. Adler, *The Geometry of Random Fields*, Society for Industrial and Applied Mathematics, doi:10.1137/1.9780898718980 (2010), https://epubs.siam.org/doi/pdf/10.1137/1.9780898718980.

[2] P. J. E. Peebles, *The Large-Scale Structure of the Universe*, Princeton University Press, ISBN 9780691209838 (1980).

[3] R. E. Angulo and O. Hahn, *Large-scale dark matter simulations*, Living Reviews in Computational Astrophysics **8**(1), 1 (2022), doi:10.1007/s41115-021-00013-z, 2112.05165.

[4] C. Rampf, *Cosmological Vlasov-Poisson equations for dark matter: Recent developments and connections to selected plasma problems*, arXiv e-prints arXiv:2110.06265 (2021), doi:10.48550/arXiv.2110.06265, 2110.06265.

[5] A. D. Chernin, D. I. Nagirner and S. V. Starikova, *Growth rate of cosmological perturbations in standard model: Explicit analytical solution*, A&A**399**, 19 (2003), doi:10.1051/0004-6361:20021763, astro-ph/0110107.

[6] Y. Brenier, U. Frisch, M. Hénon, G. Loeper, S. Matarrese, R. Mohayaee and A. Sobolevskiĭ, *Reconstruction of the early Universe as a convex optimization problem*, MNRAS**346**(2), 501 (2003), doi:10.1046/j.1365-2966.2003.07106.x, astro-ph/0304214.

[7] Y. B. Zel'dovich, *Gravitational instability: An approximate theory for large density perturbations.*, A&A**5**, 84 (1970).

[8] T. Buchert and J. Ehlers, *Lagrangian theory of gravitational instability of Friedman-Lemaitre cosmologies – second-order approach: an improved model for non-linear clustering*, MNRAS**264**, 375 (1993), doi:10.1093/mnras/264.2.375.

[9] F. R. Bouchet, S. Colombi, E. Hivon and R. Juszkiewicz, *Perturbative Lagrangian approach to gravitational instability.*, A&A**296**, 575 (1995), doi:10.48550/arXiv.astro-ph/9406013, astro-ph/9406013.

[10] C. Rampf, *The recursion relation in Lagrangian perturbation theory*, J. Cosmology Astropart. Phys.**2012**(12), 004 (2012), doi:10.1088/1475-7516/2012/12/004, 1205.5274.

[11] V. Zheligovsky and U. Frisch, *Time-analyticity of Lagrangian particle trajectories in ideal fluid flow*, Journal of Fluid Mechanics **749**, 404 (2014), doi:10.1017/jfm.2014.221, 1312.6320.

[12] T. Matsubara, *Recursive solutions of Lagrangian perturbation theory*, Phys. Rev. D**92**(2), 023534 (2015), doi:10.1103/PhysRevD.92.023534, 1505.01481.

[13] C. Rampf and O. Hahn, *Shell-crossing in a ΛCDM Universe*, MNRAS**501**(1), L71 (2021), doi:10.1093/mnrasl/slaa198, 2010.12584.

[14] M. Michaux, O. Hahn, C. Rampf and R. E. Angulo, *Accurate initial conditions for cosmological N-body simulations: minimizing truncation and discreteness errors*, MNRAS**500**(1), 663 (2021), doi:10.1093/mnras/staa3149, 2008.09588.

[15] M. Crocce, S. Pueblas and R. Scoccimarro, *Transients from initial conditions in cosmological simulations*, MNRAS**373**(1), 369 (2006), doi:10.1111/j.1365-2966.2006.11040.x, astro-ph/0606505.

[16] J. Adamek, D. Daverio, R. Durrer and M. Kunz, *General relativity and cosmic structure formation*, Nature Physics **12**(4), 346 (2016), doi:10.1038/nphys3673, 1509.01699.

[17] T. Quinn, N. Katz, J. Stadel and G. Lake, *Time stepping N-body simulations*, arXiv e-prints astro-ph/9710043 (1997), doi:10.48550/arXiv.astro-ph/9710043, astro-ph/9710043.

[18] E. Hairer, C. Lubich and G. Wanner, *Geometric numerical integration*, vol. 31 of *Springer Series in Computational Mathematics*, Springer-Verlag, Berlin, second edn., ISBN 3-540-30663-3; 978-3-540-30663-4, Structure-preserving algorithms for ordinary differential equations (2006).

[19] F. List and O. Hahn, *Perturbation-theory informed integrators for cosmological simulations*, Journal of Computational Physics **513**, 113201 (2024), doi:10.1016/j.jcp.2024.113201, 2301.09655.

[20] Y. Feng, M.-Y. Chu, U. Seljak and P. McDonald, *FASTPM: a new scheme for fast simulations of dark matter and haloes*, MNRAS**463**(3), 2273 (2016), doi:10.1093/mnras/stw2123, 1603.00476.

[21] C. Rampf, F. List and O. Hahn, *BULLFROG: multi-step perturbation theory as a time integrator for cosmological simulations*, J. Cosmology Astropart. Phys.**2025**(2), 020 (2025), doi:10.1088/1475-7516/2025/02/020, 2409.19049.

[22] M. Joyce, B. Marcos, A. Gabrielli, T. Baertschiger and F. Sylos Labini, *Gravitational Evolution of a Perturbed Lattice and its Fluid Limit*, Phys. Rev. Lett.**95**(1), 011304 (2005), doi:10.1103/PhysRevLett.95.011304, astro-ph/0504213.

[23] L. H. Garrison, D. J. Eisenstein, D. Ferrer, M. V. Metchnik and P. A. Pinto, *Improving initial conditions for cosmological N-body simulations*, MNRAS**461**(4), 4125 (2016), doi:10.1093/mnras/stw1594, 1605.02333.